05

### Synthesis and properties of the compound Na<sub>2</sub>FeLiSi<sub>6</sub>O<sub>15</sub>

© T.V. Drokina, A.M. Vorotynov, A.D. Balaev, O.A. Bayukov, M.S. Molokeev

Kirensky Institute of Physics, Federal Research Center —

Krasnoyarsk Science Center of the Siberian Branch of the Russian Academy of Sciences,

Krasnoyarsk, Russia

E-mail: tvd@iph.krasn.ru Received April 17, 2025 Revised May 25, 2025

Accepted May 27, 2025

The structural, resonance, and static magnetic properties of the  $Na_2FeLiSi_6O_{15}$  compound obtained by solid-phase synthesis from the initial oxides  $Li_2CO_3$ ,  $Na_2CO_3$ ,  $Fe_2O_3$ ,  $SiO_2$  were studied. It is shown that iron cations in emeleusite, which are in the high-spin state  $Fe^{3+}$  (S=5/2,  $3d^5$ ) and in ideal octahedra constituted by oxygen anions, in the temperature range of  $4.2-300\,\mathrm{K}$  form a paramagnetic subsystem with a molar value of the effective magnetic moment  $\mu_{\mathrm{eff}}=6.02\,\mu_{\mathrm{B}}$  and with a *g*-factor at  $T=297.8\,\mathrm{K}$  equal to 2.092. Apparently, due to the separation of iron cations by groups of non-magnetic ions  $SiO_4$ ,  $LiO_4$ , the exchange interaction between them is small (the shortest distances Fe-Fe are equal to  $5.867(3)\,\mathrm{\mathring{A}}$ ), which leads to the absence of long-range magnetic order.

**Keywords:** synthesis, crystal structure, magnetic and resonant properties.

DOI: 10.61011/PSS.2025.06.61690.83-25

### 1. Introduction

Emeleusite mineral, Na<sub>2</sub>FeLiSi<sub>6</sub>O<sub>15</sub>, was discovered in 1978 on the Island of Igdlutalik in Greenland [1]. Empirical formula of the natural mineral is Li<sub>1.91</sub>Na<sub>3.96</sub>Fe<sub>1.56</sub>Al<sub>6</sub>Ti<sub>0.07</sub>Mg<sub>0.03</sub>Zr<sub>0.01</sub>Si<sub>12</sub>O<sub>30</sub>, orthorhombic crystal structure, lattice cell parameters:  $a = 10.073 \pm 0.002$  Å,  $b = 17.350 \pm 0.005$  Å,  $c = 14.010 \pm 0.005$  Å. The number of formula units in the lattice cell is Z = 4 [1].

Results of a more complete study of the  $Na_2FeLiSi_6O_{15}$  structure are described in [2].

The objective of this study was to synthesize the  $Na_2FeLiSi_6O_{15}$  compound and investigate the structural, resonance and static magnetic properties to determine the magnetic state of a material containing  $Fe^{3+}$ .

# 2. Sample synthesis and experimental technique

 $Na_2FeLiSi_6O_{15}$  was prepared by solid-phase reaction from a stoichiometric mixture of powder-like high-purity  $Li_2CO_3,\ Na_2CO_3,\ Fe_2O_3,\ SiO_2$  with five annealing operations during 24 h at  $800-910\,^{\circ}C$  in air. The chemical and phase composition of the synthesized samples was monitored by means of X-ray diffraction analysis.

X-ray powder diffraction pattern of Na<sub>2</sub>FeLiSi<sub>6</sub>O<sub>15</sub> was recorded at room temperature using the Haoyuan DX-2700BH diffractometer (equipment of the Krasnoyarsk Regional Center of Research Equipment of the Federal Research Center — Krasnoyarsk Science Center of the Siberian Branch of the Russian Academy of

Sciences) with  $CuK_{\alpha}$  radiation and linear detector. The step size  $2\theta$  was  $0.01^{\circ}$ , the count time was — 0.2 s per step.

Nuclear gamma resonance spectra were recorded by the MS-1104Em spectrometer at the Kirensky Institute of Physics, Siberian Branch of RAS, at room temperature with a  $\text{CoCo}^{57}(\text{Rh})$  source for polycrystalline  $\text{Na}_2\text{FeLiSi}_6\text{O}_{15}$  powder samples  $5-10\,\text{mg}$  in weight per  $1\,\text{cm}^2$ , with respect to the natural iron content. Chemical shifts are given with respect to  $\alpha\text{Fe}$ .

Electron magnetic resonance spectra of NaMnFe $_2$ V $_3$ O $_{12}$  were recorded using the Bruker Elexsys E580 spectrometer in the X band within the temperature range of  $110-300\,\mathrm{K}$ . The following parameters were used for spectrum recording: microwave power —  $0.63\,\mathrm{mW}$ , modulation amplitude —  $0.7\,\mathrm{G}$ , modulation frequency —  $100\,\mathrm{kHz}$ , magnetic field sweep width —  $5\,\mathrm{kG}$ , sweep time —  $40\,\mathrm{s}$ .

Static magnetic properties of Na<sub>2</sub>FeLiSi<sub>6</sub>O<sub>15</sub> were measured using the Quantum Design PPMS-9 (Physical Property Measurement System) within the temperature range of  $1.8 \leq T \leq 300 \, \text{K}$ .

### 3. Experimental results and discussion

### 3.1. Structural investigation data

Structural properties of the polycrystalline Na<sub>2</sub>FeLiSi<sub>6</sub>O<sub>15</sub> compound were examined by the X-ray diffraction and Mössbauer spectroscopy methods.

Figure 1 shows an X-ray powder diffraction pattern of Na<sub>2</sub>FeLiSi<sub>6</sub>O<sub>15</sub> at room temperature.

Rietveld refinement was implemented in TOPAS 4.2 [3]. Almost all peaks, except small peaks of the NaFeSi<sub>2</sub>O<sub>6</sub>

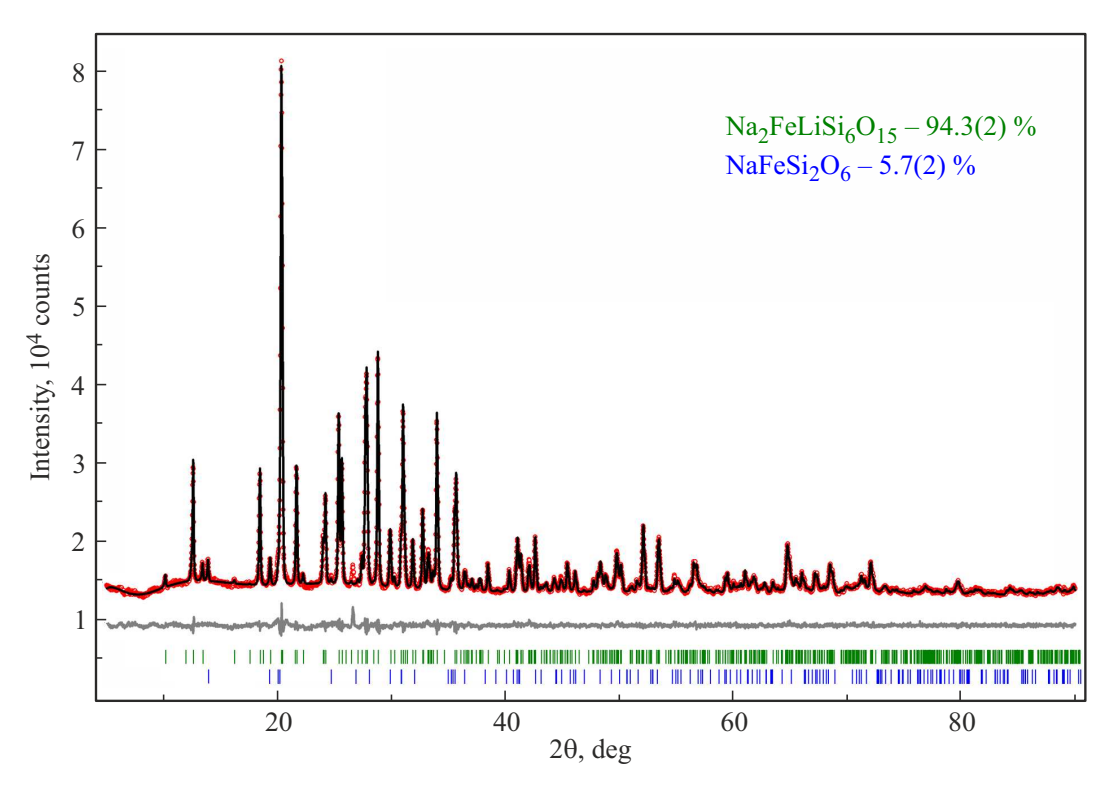


Figure 1. X-ray pattern of the polycrystalline  $Na_2FeLiSi_6O_{15}$  compound at  $T=300\,\mathrm{K}$ . Differential X-ray diffraction pattern is the lower curve.

Phase	Concentration, %	Space group	Cell parameters, Å, deg.; cell volume, Å <sup>3</sup>	$R_{\text{wp}}, R_{\text{p}}, \%;$ $\chi^2$	$R_{\mathrm{B}}$ , %
Na <sub>2</sub> FeLiSi <sub>6</sub> O <sub>15</sub>	94.3(2)	Стса	a = 14.0260(2), b = 17.3867(3), c = 10.0918(2), V = 2461.05(8)	1.29,	0.39
NaFeSi <sub>2</sub> O <sub>6</sub>	5.7(2)	C2/c	a = 9.656(1), b = 8.7974(1), c = 5.2939(6), $\beta = 107.708(9),$ V = 428.41(9)	0.96, 1.61	0.62

Table 1. Main parameters of the X-ray experiment and results of Na<sub>2</sub>FeLiSi<sub>6</sub>O<sub>15</sub> crystalline structure confirmation

Note:  $a, b, c, \beta$  — lattice cell parameters; V — cell volume; uncertainty factors:  $R_p$  — profile factor,  $R_B$  — integral factor; and  $\chi^2$  – the quality of fit.

impurity (5.7(2) wt.%), are described by an orthorhombic cell (Cmca) with parameters close to those of Na<sub>2</sub>FeLiSi<sub>6</sub>O<sub>15</sub> [2] (garnet type structure). Thus, the Na<sub>2</sub>FeLiSi<sub>6</sub>O<sub>15</sub> structure was used as an initial model for the Rietveld refinement. Nonstandard space group Acam was reduced to standard space group Cmca, atom coordinates were transformed according to the changes. The refinement was stable and exhibited low R-factors (Table 1 and Figure 1).

The number of formula units in the lattice cell is Z=8. Atom coordinates in the crystalline Na<sub>2</sub>FeLiSi<sub>6</sub>O<sub>15</sub> structure, population of positions and thermal parameters are listed in Table 2.

Main bond distances in the crystalline structure at  $T = 300 \,\mathrm{K}$  are listed in Table 3.

The compound structure is shown in Figure 2.

Crystalline  $Na_2FeLiSi_6O_{15}$  structure is a multilayer structure parallel to (001). It consists of zigzag double silicate chains extended along the [100] axis, that are connected by Na(2) polyhedra chains and alternating Li tetrahedra and Fe octahedra. Na(1) atom is located in a mirror plane coordinated by nine oxygen atoms. A plane containing Li, Fe and Na(2) atoms is placed parallel to double silicate chains. Li tetrahedra and Fe octahedra have common edges O(2)-O(4) forming the chains in the [001] orientation.

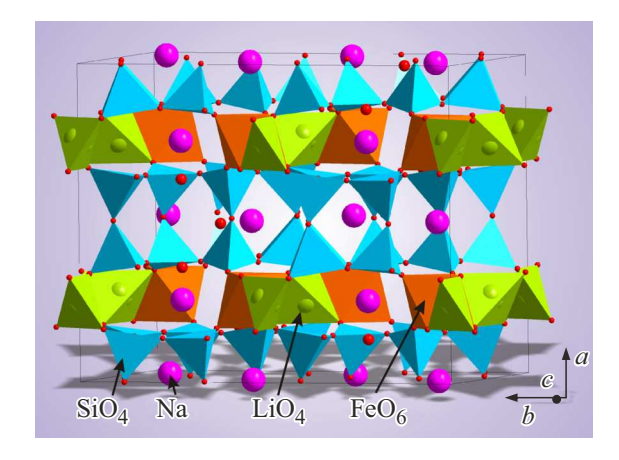


Figure 2. Crystalline structure of Na<sub>2</sub>FeLiSi<sub>6</sub>O<sub>15</sub>.

The state of iron cations in Na<sub>2</sub>FeLiSi<sub>6</sub>O<sub>15</sub> was studied by the nuclear  $\gamma$ -resonance method. The Mössbauer spectrum measured at room temperature is shown in Figure 3, a. Quadrupole splitting distribution in the experimental spectrum is shown in Figure 3, b. Spectrum parameters are listed in Table 4.

It follows from the Mössbauer spectroscopy data that iron cations in the sample phases are in the high-spin state  $Fe^{3+}$  (S = 5/2,  $3d^5$ ) and in coordination 6 with respect to

**Table 2.** Atom coordinates, isotropic thermal parameters Biso in the crystalline  $Na_2FeLiSi_6O_{15}$  structure at  $T=300\,\mathrm{K}$ 

Atom	x	у	z	$B_{\rm iso}$ , Å <sup>2</sup>
Na1	0.5	0.4143(5)	0.2504(6)	2.5(2)
Na2	0.25	0.2252(3)	0.25	2.3(2)
Li	0.245(5)	0	0	1.6(8)
Fe	0.25	0.4139(2)	0.25	1.47(15)
Si1	0.6131(5)	0.1329(2)	0.4845(4)	0.96(13)
Si2	0.6130(3)	0.0727(3)	0.1914(3)	0.96(13)
Si3	0.6139(4)	0.3096(2)	0.4579(3)	0.96(13)
O1	0.1384(6)	0.2232(5)	-0.0030(5)	0.50(14)
O2	0.1681(4)	0.4190(4)	0.4168(8)	0.50(14)
О3	0.3621(6)	0.1119(3)	0.3338(7)	0.50(14)
O4	0.3333(5)	0.4934(4)	0.3367(8)	0.50(14)
O5	0.3581(7)	0.1398(4)	0.0860(7)	0.50(14)
O6	0.1639(4)	0.3322(4)	0.1726(7)	0.50(14)
O7	0.5	0.1207(5)	0.5130(9)	0.50(14)
O8	0.5	0.0542(5)	0.1865(8)	0.50(14)
О9	0.5	0.3211(5)	0.4387(9)	0.50(14)

**Table 3.** Main bond distances in the crystalline Na<sub>2</sub>FeLiSi<sub>6</sub>O<sub>15</sub> structure at  $T=300\,\mathrm{K}$ 

Bond	Distance, Å	Bond	Distance, Å
Na1-O2i	2.901(8)	Fe-O2	2.039(7)
Na1-O4	2.850(8)	Fe-O4	2.010(8)
Na1-O6 <sup>i</sup>	2.815(8)	Fe-O6	2.022(7)
Na1-O7 <sup>ii</sup>	2.471(11)	Si1-O1 <sup>vii</sup>	1.621(9)
Na1-O8 <sup>iii</sup>	2.516(12)	Si1-O2 <sup>viii</sup>	1.551(9)
Na1-O9	2.497(11)	Si1-O3 <sup>ix</sup>	1.603(8)
Na2-O1	2.995(6)	Si1-O7	1.626(7)
Na2-O1 <sup>iv</sup>	3.077(7)	Si2-O3 <sup>ix</sup>	1.627(8)
Na2-O3	2.658(8)	Si2-O4 <sup>x</sup>	1.597(8)
Na2-O5	2.691(8)	Si2-O5 <sup>ix</sup>	1.630(8)
Na2-O6	72.353(8)	Si2-O8	1.618(4)
Li-O <sup>v</sup>	1.96(4)	Si3-O1 <sup>vii</sup>	1.606(9)
Li-O3 <sup>vi</sup>	2.97(4)	Si3-O5 <sup>xi</sup>	1.613(8)
Li-O4 <sup>v</sup>	2.07(4)	Si3-O6 <sup>vii</sup>	1.543(8)
Li-O5	3.03(4)	Si3-O9	1.622(6)

Symmetry Codes: (i) -x + 1/2, y, -z + 1/2; (ii) -x + 1, -y + 1/2, z - 1/2; (iii) -x + 1, y + 1/2, -z + 1/2; (iv) -x + 1/2, -y + 1/2, -z; (v) x, -y + 1/2, z - 1/2; (vi) -x + 1/2, -y, z - 1/2; (vii) x + 1/2, y, -z + 1/2; (viii) x + 1/2, -y + 1/2, -z + 1; (ix) -x + 1, y, z; (x) -x + 1, y - 1/2, -z + 1/2; (xi) -x + 1, -y + 1/2, -z + 1/2.

oxygen. For the main  $Na_2FeLiSi_6O_{15}$  phase, quadrupole splitting QS  $(0.23\,\text{mm/s})$  is much smaller than the line width W, which indicates that iron cations are in ideal octahedra formed by oxygen anions.

The NaFeSi $_2$ O $_6$  impurity phase has very wide absorption lines (0.90 mm/s), which is probably due to distortion of the aegirine crystal structure.

### 3.2. EPR examination results for Na<sub>2</sub>FeLiSi<sub>6</sub>O<sub>15</sub>

Electron paramagnetic resonance (EPR) spectra in  $Na_2FeLiSi_6O_{15}$  were studied at 9 GHz in the temperature range of  $110-300\,\mathrm{K}$ . Figure 4 shows the EPR spectrum at room temperature and fitting of the experimental EPR spectrum by two Lorentzian-shaped absorption curves 1 and 2.

Figure 5 shows the temperature dependences of the intensity I, resonance field  $H_{\rm res}$  and line width dH for fitting curves I and 2. The intensity was defined as the area under the EPR signal fitting lines, the line width was defined as a distance in the field between the extrema on the absorption line derivative curve, the resonance field value corresponded to the intersection between the first absorption derivative curve and zero line.

**Table 4.** Mössbauer parameters if  ${}^{57}$ Fe in Na<sub>2</sub>FeLiSi<sub>6</sub>O<sub>15</sub>: IS — isomeric chemical shift with respect to  $\alpha$ -Fe, QS — quadrupole splitting, W — absorption line width, A — population of iron position on the assumption of the same probability of the Mössbauer effect for various crystallographic positions

IS, mm/s ±0.01	QS, mm/s ±0.02	$W$ , mm/s $\pm 0.02$	A, at.% $\pm 5$	Position
0.41	0.23	0.39	61	Fe <sup>3+</sup> (6) in Na <sub>2</sub> FeLiSi <sub>6</sub> O <sub>15</sub>
0.39	0.67	0.90	39	Fe <sup>3+</sup> (6) in NaFeSi <sub>2</sub> O <sub>6</sub>

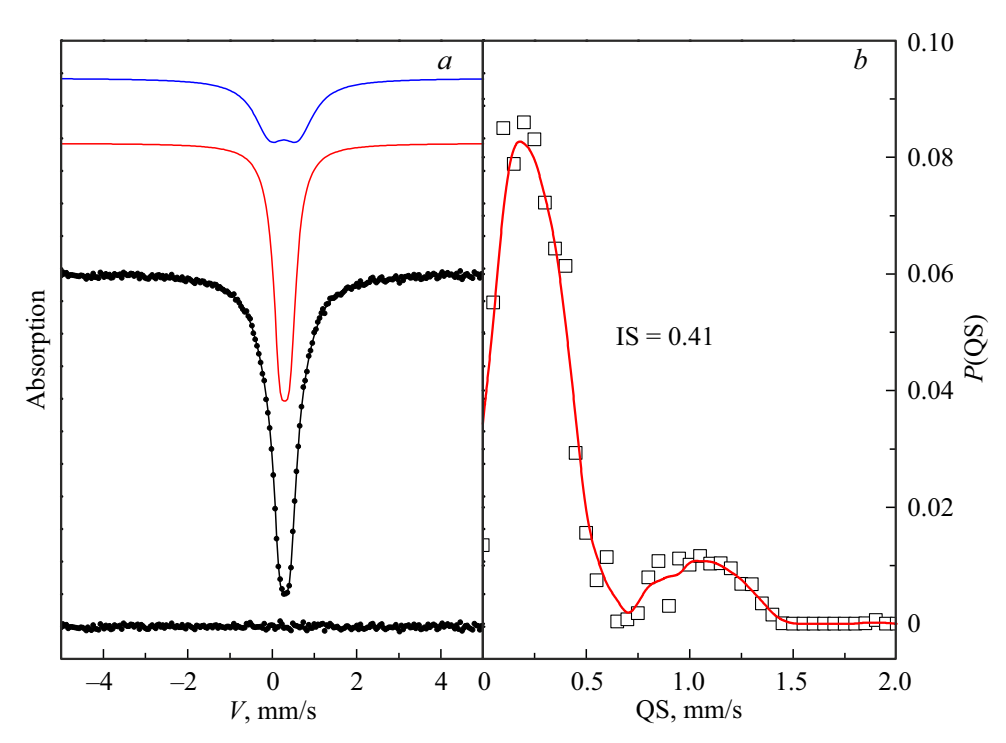


**Figure 3.** a) Mössbauer spectrum of  $Na_2FeLiSi_6O_{15}$  measured at room temperature. Colored lines denote the spectrum components. Below the spectrum, there is an error spectrum (difference between the experimental and theoretical spectra). b) Distribution of quadrupole splittings in the experimental spectrum.

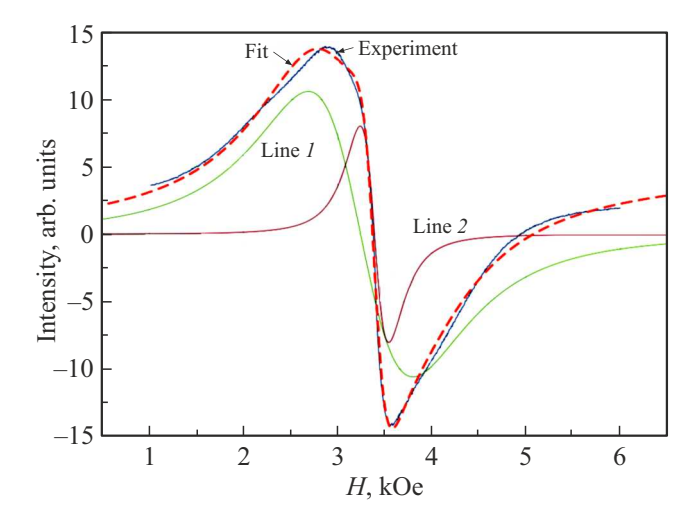


**Figure 4.** EPR spectrum of  $Na_2FeLiSi_6O_{15}$  at 9 GHz at room temperature and fitting of the experimental spectrum by two Lorentzian-shaped absorption curves  $\it I$  and  $\it 2$ .

It follows from the EPR data analysis that signal I is induced by the main Na<sub>2</sub>FeLiSi<sub>6</sub>O<sub>15</sub> matrix. Signal 2 is given by the NaFeSi<sub>2</sub>O<sub>6</sub> phase. At  $T=297.8\,\mathrm{K}$ , the Lande g-actors for curves I and 2 are g(1)=2.092 and g(2)=1.995, respectively. At  $T=108\,\mathrm{K}$  g(1)=2.167 and g(2)=2.021.

## 3.3. Results of static magnetic measurements of Na<sub>2</sub>FeLiSi<sub>6</sub>O<sub>15</sub>

Magnetic atom in Na<sub>2</sub>FeLiSi<sub>6</sub>O<sub>15</sub> is an iron cation in the high-spin state Fe<sup>3+</sup>  $(S=5/2,\,L=0)$  in the octahedral oxygen environment.

Figure 6 shows the temperature dependences of the magnetic moment M and inverse magnetic susceptibility of  $\chi^{-1}$  Na<sub>2</sub>FeLiSi<sub>6</sub>O<sub>15</sub> measured in the magnetic field H = 1000 Oe (sample weight m = 0.06353 g).

The sample contains the  $NaFeSi_2O_6$  impurity phase. Structural and magnetic properties of aegirine are reported

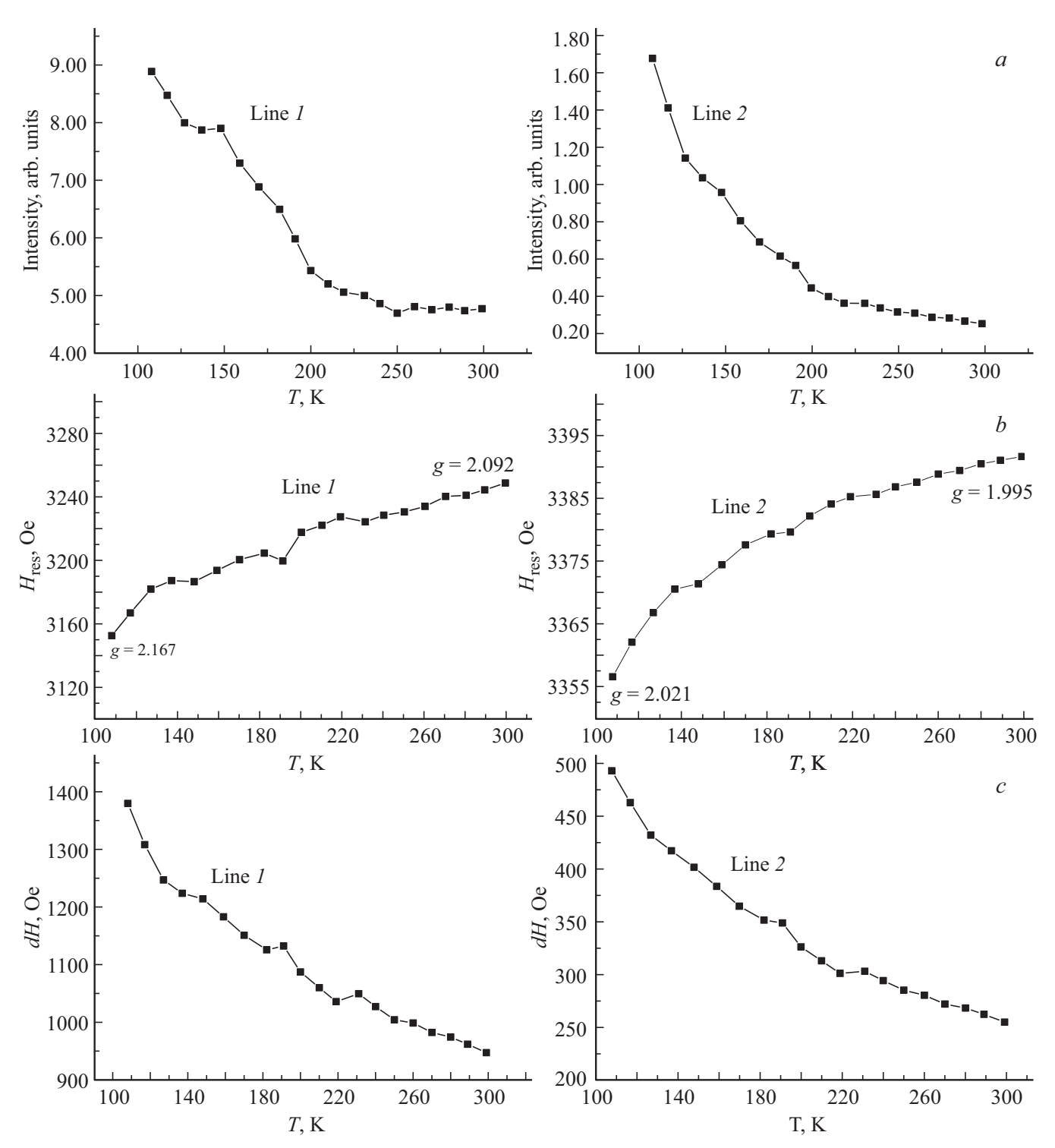


**Figure 5.** Temperature dependences of a) intensity I, b) resonance field  $H_{\rm res}$ , c) EPR signal line width dH at  $\nu = 9$  GHz in Na<sub>2</sub>FeLiSi<sub>6</sub>O<sub>15</sub>.

in [4–9]. Crystalline symmetry is described by monoclinic space group C2/c. The number of formula units in the lattice cell is Z=4.

Magnetic atom in the NaFeSi<sub>2</sub>O<sub>6</sub> impurity compound is also an iron cation in the high-spin state Fe<sup>3+</sup> (S = 5/2) in

the octahedral oxygen environment. Polyhedra around Fe atoms in the impurity of our sample are heavily distorted (quadrupole splitting  $Q = 1.00 \, \text{mm/s}$ ), Table 4.

At high temperatures in clinopyroxene, NaFeSi<sub>2</sub>O<sub>6</sub>, paramagnetic state described by the Curie–Weiss law

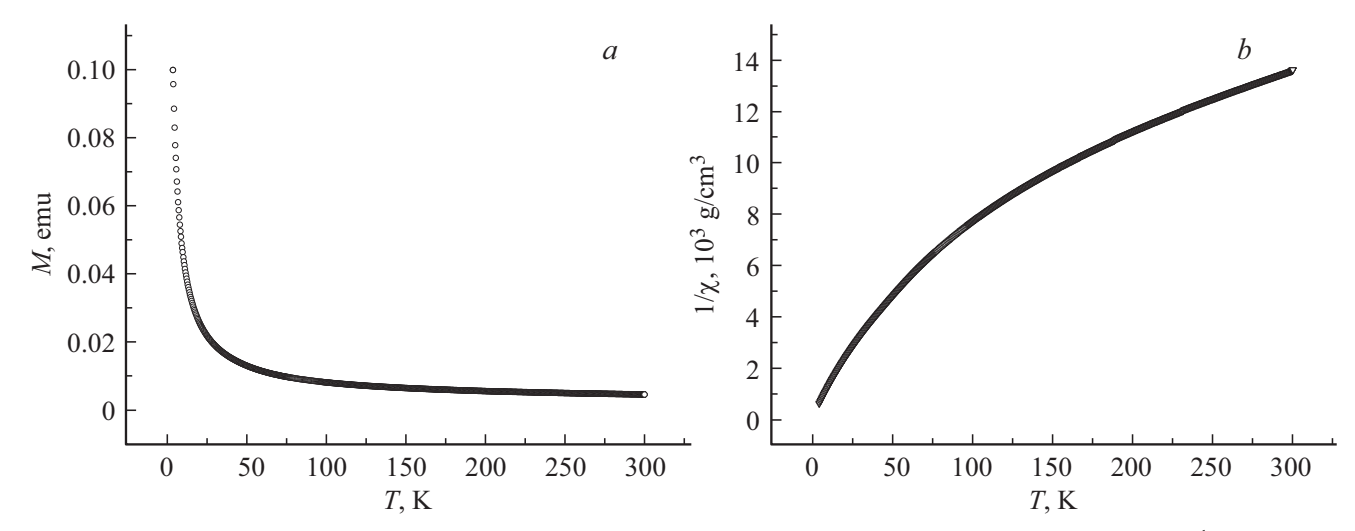


**Figure 6.** Temperature dependences of a) magnetic moment M and b) and inverse magnetic susceptibility of  $\chi^{-1}$  Na<sub>2</sub>FeLiSi<sub>6</sub>O<sub>15</sub> measured in the magnetic field H = 1000 Oe (sample weight m = 0.06353 g).

with the asymptotic Néel temperature  $\Theta = -43.6 \, \text{K}$ ,  $C = 0.0166 \, \text{K} \cdot \text{cm}^3/\text{g}$  and  $\mu_{\text{eff}} = 5.56 \, \mu_{\text{B}}$  is implemented [8]. At  $T_{\text{N}} = 7.8 \, \text{K}$ , the sample switches from the paramagnetic state to a state with long-range magnetic order, including commensurable and incommensurable modulated magnetic structures that are formed primarily by antiferromagnetic interaction [9].

To determine magnetic properties of  $Na_2FeLiSi_6O_{15}$ , the fitting function was used for the temperature dependence of magnetic susceptibility recorded as follows:

$$\chi(T) = \chi_0 + 0.943C/(T - \Theta) + 0.057 \cdot 0.0166/(T + 43.6),$$

where  $\chi_0$  are temperature-independent Van Vleck paramagnetism contribution and diamagnetic contribution, C and T are fitting parameters of the main Na<sub>2</sub>FeLiSi<sub>6</sub>O<sub>15</sub> phase. The third term in the equation is contribution to susceptibility from the NaFeSi<sub>2</sub>O<sub>6</sub> impurity phase with parameters taken from [8]. Processing of the magnetic susceptibility dependence in emeleusite, Na<sub>2</sub>FeLiSi<sub>6</sub>O<sub>15</sub>, considers the X-ray diffraction analysis data for phase content, Table 1. The result is shown in Figure 7.

The following parameters were eventually obtained for the main Na<sub>2</sub>FeLiSi<sub>6</sub>O<sub>15</sub> phase  $C = 0.00871 \,\mathrm{K \cdot cm^3/g}$  $\Theta = -3.01 \,\mathrm{K}$  $\chi_0$ :  $\chi_0 = 4.45688 \cdot 10^{-5} \,\mathrm{cm}^3/\mathrm{g}$ . C corresponds to the molar effective magnetic moment  $\mu_{\text{eff}} = 6.02 \,\mu_{\text{B}}$ .

Magnetic susceptibility  $\chi$  in Na<sub>2</sub>FeLiSi<sub>6</sub>O<sub>15</sub> depends on T according to the hyperbolic law (Figure 7), which is typical of paramagnetic state. As the temperature increases, the magnetic susceptibility decreases due to thermal motion leading to disordered magnetic moment arrangement. Due to the separation of iron cations by the nonmagnetic ion groups (SiO<sub>4</sub>, LiO<sub>4</sub>), the exchange interaction between them is probably low (the shortest distances Fe–Fe are 5.867(3) Å).

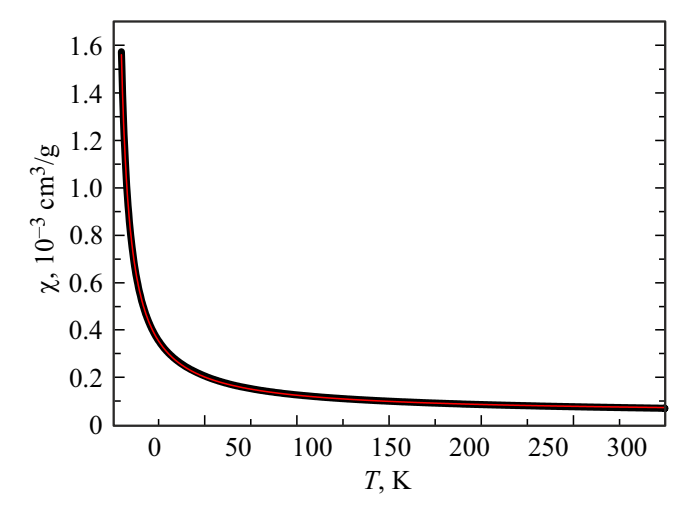


**Figure 7.** Temperature dependence of the magnetic susceptibility  $\chi$  of Na<sub>2</sub>FeLiSi<sub>6</sub>O<sub>15</sub>. Black line — experiment, red line — fitting curve.

### 4. Conclusion

Emeleusite,  $Na_2FeLiSi_6O_{15}$ , was prepared by solid-phase reaction from a stoichiometric mixture of powder-like high-purity  $Li_2CO_3$ ,  $Na_2CO_3$ ,  $Fe_2O_3$ ,  $SiO_2$  with five annealing operations at  $800-910\,^{\circ}C$ . The paper describes the X-ray diffraction, electron paramagnetic resonance, nuclear gamma resonance and static magnetic measurement data concerning the properties of the synthesized compound.

Crystalline Na<sub>2</sub>FeLiSi<sub>6</sub>O<sub>15</sub> structure is described by the orthorhombic cell, space group *Cmca*, with parameters close to those of the natural mineral.

It is shown that emeleusite is a paramagnetic material with molar effective magnetic moment  $\mu_{\rm eff} = 6.02 \, \mu_{\rm B}$  and *g*-factor at T = 297.8 K, equal to 2.092.

### **Acknowledgments**

The authors are grateful to the Krasnoyarsk Regional Shared Access Center of the Federal Research Center "Krasnoyarsk Science Center of the Siberian Branch of the Russian Academy of Sciences" for providing the X-ray diffraction and EPR measurement equipment.

### **Funding**

The study was carried out within the range of research topics under the state assignment of the Kirensky Institute of Physics, SB RAS.

#### Conflict of interest

The authors declare no conflict of interest.

### References

- B.G.J. Upton, P.G. Hill, O. Johnsen, O.V. Petersen. Mineral. Mag. 42, 321, 31 (1978).
- [2] O. Johnsen, K. Nielsen, I. Sotofte. Z. Kristallogr. Cryst. Mater. 147, 297 (1978).
- [3] Bruker AXS TOPAS V4: General profile and structure analysis software for powder diffraction data. User's Manual. Bruker AXS, Karlsruhe, Germany (2008).
- [4] O. Ballet, J.M.D. Coey, G. Fillion, A. Ghose, A. Hewat, J.R. Regnard. Phys. Chem. Minerals 16, 7, 672 (1989).
- [5] E. Baum, W. Treutmann, W. Lottermoser, G. Amthauer. Phys. Chem. Minerals 24, 4, 294 (1997).
- [6] G.J. Redhammer, G. Amthauer, W. Lottermoser, W. Treutmann. Eur. J. Mineral 12, 1-2, 105 (2000).
- [7] S. Jodlauk, P. Becker, J.A. Mydosh, D.I. Khomskii, T. Lorenz, S.V. Streltsov, D.C. Hezel, L. Bohaty. J. Phys.: Condens. Matters 19, 43, 432201 (2008).
- [8] S.V. Streltsov, D.I. Khomskii. Phys. Rev. B77, 6, 064405 (2007).
- [9] G.J. Redhammer, A. Senyshyn, M. Meven, G. Roth, S. Prinz, A. Pachler, G. Tippelt, C. Pietzonka, W. Treutmann, M. Hoelzel, B. Pedersen, G. Amthauer. Phys. Chem. Minerals 38, 2, 139 (2010).

Translated by E.Ilinskaya